Supporting Materials

Asymmetric Schottky Barrier-Generated MoS2/WTe2 FET Biosensor Based on a Rectified Signal

Xinhao Zhang [1,†], Shuo Chen [1,†], Heqi Ma [1], Tianyu Sun [1], Xiangyong Cui [1], Panpan Huo [1], Baoyuan Man [1,*] and Cheng Yang [1,2,*]

[1] School of Physics and Electronics, Shandong Normal University, Jinan 250014, China; zhangxh0050@163.com (X.Z.); 1091471811@qq.com (S.C.); 1005740998@qq.com (H.M.); 377633468@qq.com (T.S.); 2199491415@qq.com (X.C.); ghost54051@qq.com (P.H.)

[2] Shandong Provincial Engineering and Technical Center of Light Manipulations, Shandong Normal University, Jinan 250014, China

* Correspondence: byman@sdnu.edu.cn (B.M.); chengyang@sdnu.edu.cn (C.Y.)

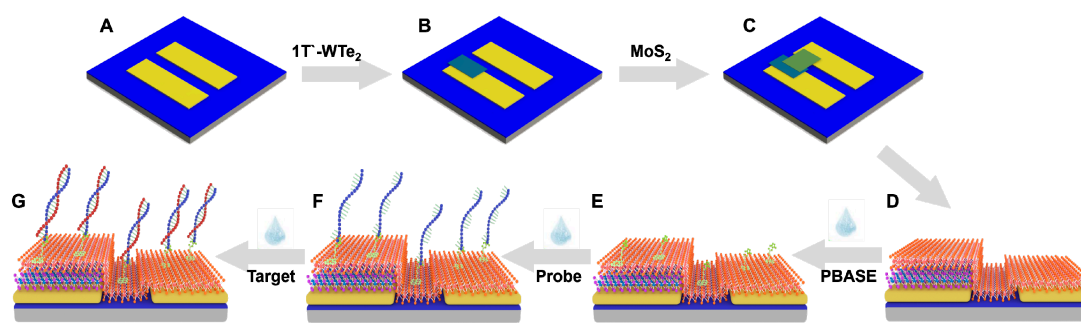† These authors contributed equally to this work.

Figure S1. Fabrication process diagram of MoS₂/WTe₂ FET biosensor. (A) A clean and tidy Si/SiO₂ substrate is prepared. (B) WTe₂ is transferred by using a two-dimensional material transfer platform. (C) MoS₂ is transferred by using a two-dimensional material transfer platform. (D) A MoS₂/WTe₂ Schottky heterojunction is formed. (E) Add PBASE on the MoS₂/WTe₂ FET biosensor. (F) Add probe DNA on the MoS₂/WTe₂ FET biosensor. (G) Add target DNA on the MoS₂/WTe₂ FET biosensor.
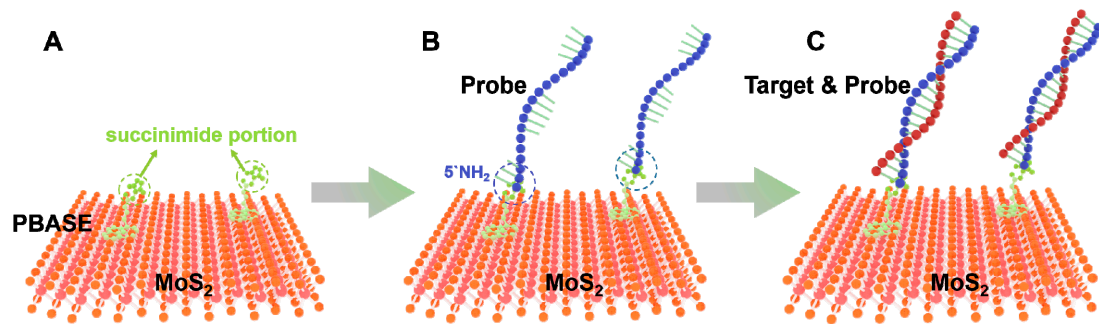
Figure S2. The functionalization and immobilization process of the device. (A) PBASE, when dissolved in DMSO, stacks its pyrene group on the surface of MoS2, binds to MoS2. (B) The succinimidyl ester group of PBASE is connected to the amino-modified probe DNA through a cross-linking reaction. (C) The target DNA is combined with the probe DNA through complementary base pairing.
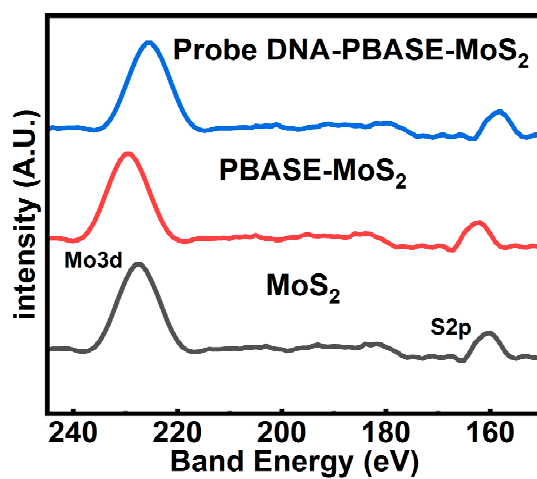
Figure S3. High-resolution XPS spectra of Mo 3d, S 2p. The movement of Mo 3d peak and S 2p peak confirmed that PBASE and probe DNA were successfully combined on the surface of MoS_2/WTe_2 FET biosensor.
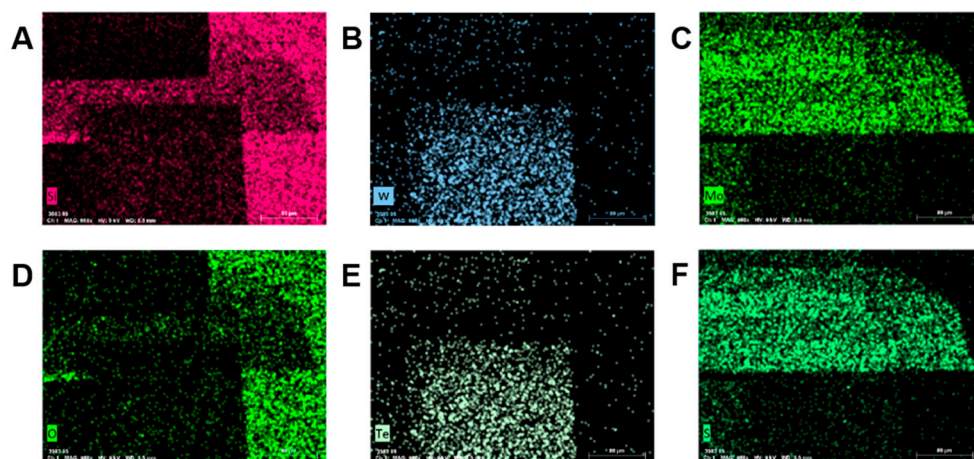
Figure S4. EDS images mentioned in Figure 3B. The above EDS images represent (A) Si, (B) W, (C) Mo, (D) O, (E) Te and (F) S elements respectively.
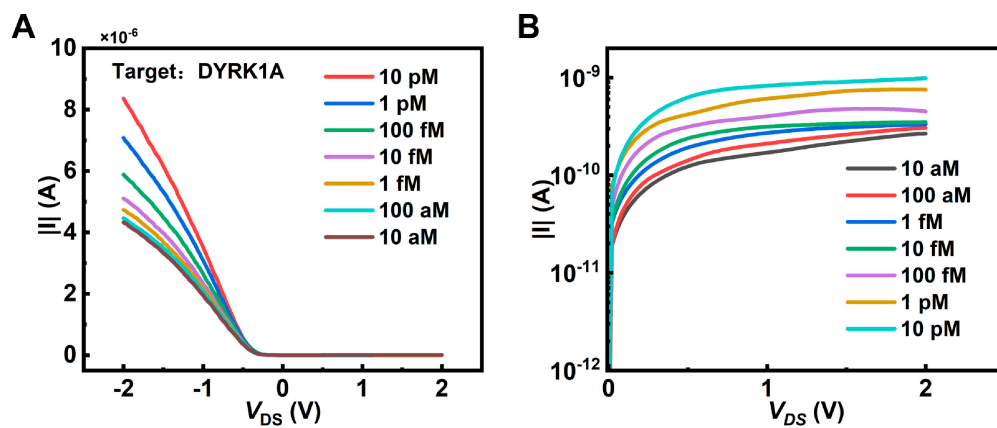
Figure S5. The current results of different concentrations of target DNA (DYRK1A) under (A) positive and (B) negative bias voltages.
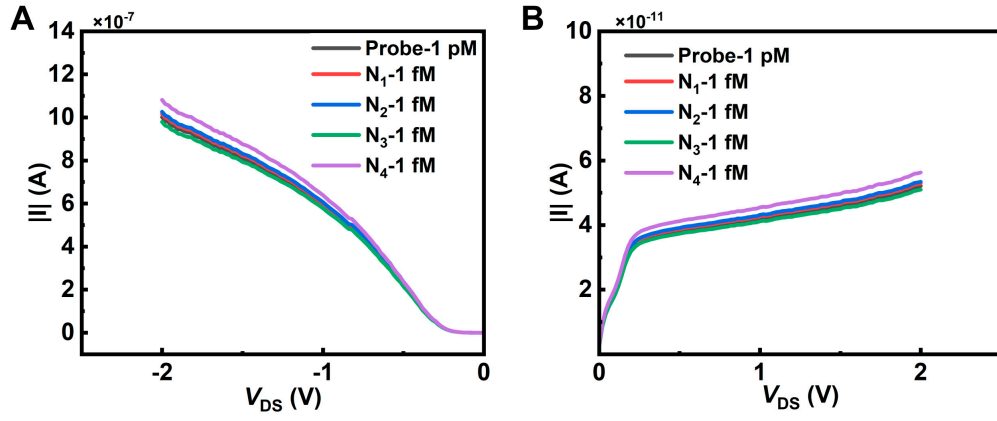
Figure S6. The complete current diagram after adding N_1-N_4 samples. Source-drain current under (A) negative bias and (B) positive bias in linear scale.
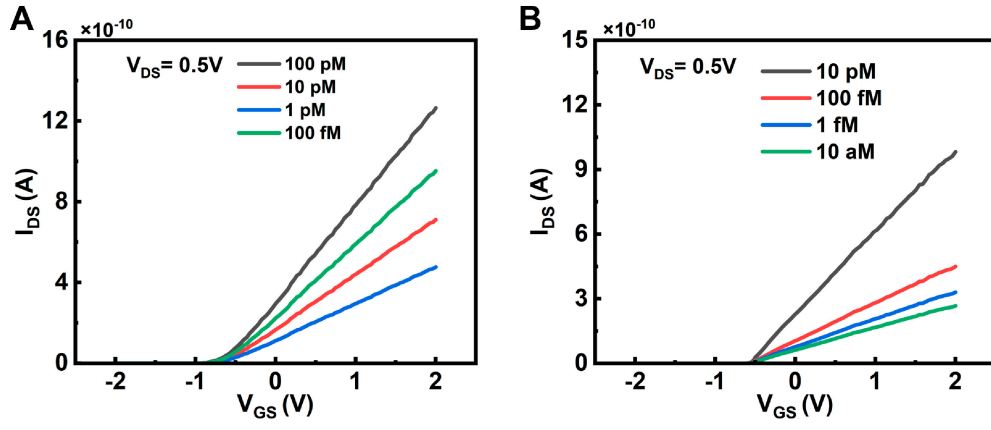
Figure S7: The transfer characteristics curves of the (A) Au/MoS₂/Au and (B) WTe₂/MoS₂/Au structures, respectively.
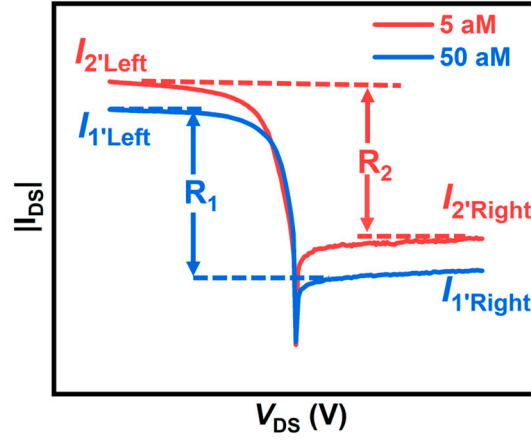
Figure S8. Output characteristics curves measured at different biomolecular concentrations in the MoS$_2$/WTe$_2$ FET biosensor. I$_1$ and I$_2$ respectively represent the source-drain current at different concentrations, I$_{Left}$ and I$_{Right}$ respectively represent the source-drain current dominated by different Schottky barriers, R$_1$ and R$_2$ respectively represent the rectification ratio of MoS$_2$/WTe$_2$ FET biosensor at different concentrations
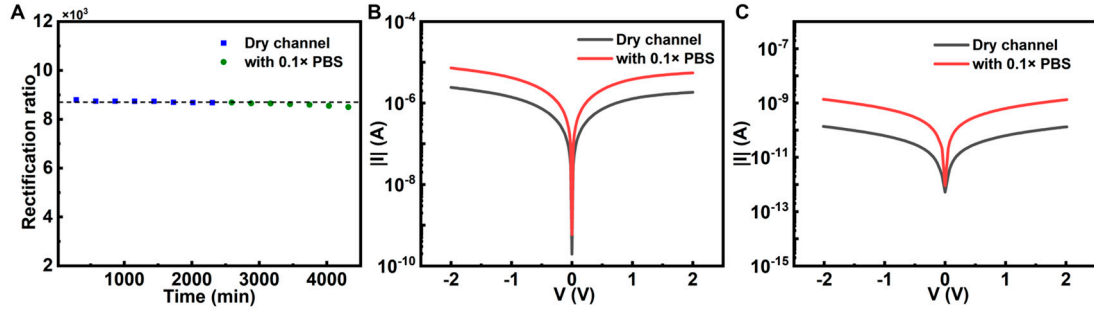
Figure S9. Stability comparison of "rectified signal" and "absolute value signal". The output current curves of (A) WTe₂/MoS₂/Au FET, (B) WTe₂/MoS₂/WTe₂ FET, and (C) Au/MoS₂/Au FET under external factors such as water molecules, respectively. Under external factors such as water molecules, the rectification ratio signal of the WTe₂/MoS₂/Au FET biosensor is stable within long times, as shown in Supplementary Figure 3A.

Table S1. The DNA sequences purchased from Sangon Biotech (Shanghai) Co., Ltd

Names	Sequences (5'→3')
Probe DNA in Figs. 1B-1C, 1H-1I, 2I, 3B-3F	NH_2-C_6-CAGAGTCACTGACTCACTA
Target DNA in Figs. 1C,1I,2I,2B-2D	TTAGTGAGTCAGTGACTCTG
RNA in Figs. 3F-3G	CAGGUGGAACCUCAUCAGGAGAUGC
T1 in Figs. 3F-3G	TTTTTTTTTTUUUUUUCCCGTCCGTATGG
T2 in Figs. 3F-3G	TCTCAAGGACCACCGCATCTCTACCCATAC GGACGGG
3-base Mismatch DNA in Figs. 3F-3G	TTAGTGAGTCAGTGACTGAC

Target DNA sequence in Figs. 1C,1I,2I,2B-2D was selected from GeneBank: NG_009366.2

Table S2. Comparison of biosensing performance among various FET biosensors

Sensing materials	Functionalization methods	Probe types	Target biomarkers	LOD	Signal types	Ref
Graphene	PBASE	ssDNA	Antigen	2.6 pM	V_{Dirac}; I_{DS}	[1]
rGO	PBASE	Antibody	Antigen	0.1 pg/mL	V_{Dirac}	[2]
Graphene	AuNPs	ssDNA	20-mer DNA	15 aM	V_{CNP}	[3]
Mxenes/graphene	APTES	Antibody	Antigen	1 fg/mL	V_G; I_{DS}	[4]
MoS$_2$	Physically adsorb	Antibody	Antigen	1 pM	V_{th}	[5]
MoS$_2$	AuNPs	ssDNA	30-mer DNA	10 aM	I_{DS}	[6]
rGO	Physically adsorb	ssDNA	48-mer DNA	5 pM	I_{DS}	[7]

Exfoliated-Graphene	EDC+NHS	Antibody	Antigen	10 fg/mL	Resistance	[8]
MoS_2/WTe_2	PBASE	ssDNA	20-mer DNA	10 aM	Rectification ratio	This work

References

1. Khan, N.I.; Mousazadehkasin, M.; Ghosh, S.; Tsavalas, J.G.; Song, E. An integrated microfluidic platform for selective and real-time detection of thrombin biomarkers using a graphene FET. *Analyst* **2020**, *145*, 4494-4503.

2. Park, D.; Kim, J.H.; Kim, H.J.; Lee, D.; Lee, D.S.; Yoon, D.S.; Hwang, K.S. Multiplexed femtomolar detection of Alzheimer's disease biomarkers in biofluids using a reduced graphene oxide field-effect transistor. *Biosens. Bioelectron.* **2020**, *167*, 112505.

3. Danielson, E.; Sontakke, V.A.; Porkovich, A.J.; Wang, Z.; Kumar, P.; Ziadi, Z.; Yokobayashi, Y.; Sowwan, M. Graphene based field-effect transistor biosensors functionalized using gas-phase synthesized gold nanoparticles. *Sens. Actuators. B: Chem* **2020**, *320*, 128432.

4. Li, Y.; Peng, Z.; Holl, N.J.; Hassan, M.R.; Pappas, J.M.; Wei, C.; Izadi, O.H.; Wang, Y.; Dong, X.; Wang, C. MXene–graphene field-effect transistor sensing of influenza virus and SARS-CoV-2. *ACS omega* **2021**, *6*, 6643-6653.

5. Park, H.; Lee, H.; Jeong, S.H.; Lee, E.; Lee, W.; Liu, N.; Yoon, D.S.; Kim, S.; Lee, S.W. MoS2 field-effect transistor-amyloid-β1–42 hybrid device for signal amplified detection of MMP-9. *Anal. Chem.* **2019**, *91*, 8252-8258.

6. Liu, J.; Chen, X.; Wang, Q.; Xiao, M.; Zhong, D.; Sun, W.; Zhang, G.; Zhang, Z. Ultrasensitive monolayer MoS2 field-effect transistor based DNA sensors for screening of down syndrome. *Nano Lett.* **2019**, *19*, 1437-1444.

7. Chan, C.; Shi, J.; Fan, Y.; Yang, M. A microfluidic flow-through chip integrated with reduced graphene oxide transistor for influenza virus gene detection. *Sens. Actuators. B: Chem* **2017**, *251*, 927-933.

8. Islam, S.; Shukla, S.; Bajpai, V.K.; Han, Y.-K.; Huh, Y.S.; Kumar, A.; Ghosh, A.; Gandhi, S. A smart nanosensor for the detection of human immunodeficiency virus and associated cardiovascular and arthritis diseases using functionalized graphene-based transistors. *Biosens. Bioelectron.* **2019**, *126*, 792-799.